

000 ORACLEAGENT: A MULTIMODAL REASONING AGENT 001 FOR ORACLE BONE SCRIPT RESEARCH 002 003 004

005 **Anonymous authors**

006 Paper under double-blind review

007 008 ABSTRACT 009 010

011 As one of the earliest writing systems, Oracle Bone Script (OBS) preserves the
012 cultural and intellectual heritage of ancient civilizations. However, current OBS
013 research faces two major challenges: (1) the interpretation of OBS involves a com-
014 plex workflow comprising multiple serial and parallel sub-tasks, and (2) the effi-
015 ciency of OBS information organization and retrieval remains a critical bottleneck,
016 as scholars often spend substantial effort searching for, compiling, and managing
017 relevant resources. To address these challenges, we present **OracleAgent**, the
018 first agent system designed for the structured management and retrieval of OBS-
019 related information. OracleAgent seamlessly integrates multiple OBS analysis
020 tools, empowered by large language models (LLMs), and can flexibly orchestrate
021 these components. Additionally, we construct a comprehensive domain-specific
022 multimodal knowledge base for OBS, which is built through a rigorous multi-
023 year process of data collection, cleaning, and expert annotation. The knowledge
024 base comprises over **1.4M** single-character rubbing images and **80K** interpretation
025 texts. OracleAgent leverages this resource through its multimodal tools to assist
026 experts in retrieval tasks of character, document, interpretation text, and rubbing
027 image. Extensive experiments demonstrate that OracleAgent achieves superior
028 performance across a range of multimodal reasoning and generation tasks, sur-
029 passing leading mainstream multimodal large language models (MLLMs) (e.g.,
030 *GPT-4o*). Furthermore, our case study illustrates that OracleAgent can effectively
031 assist domain experts, significantly reducing the time cost of OBS research. These
032 results highlight OracleAgent as a significant step toward the practical deployment
033 of OBS-assisted research and automated interpretation systems.

034 035 1 INTRODUCTION 036 037

038 Oracle Bone Script (OBS) is the earliest known form of the Chinese writing system, dating back
039 more than 3,000 years to the Shang Dynasty (c. 1400–1100 B.C.). Inscribed on turtle plastrons
040 and animal scapulae for divination, ritual, and record-keeping, these inscriptions not only document
041 major historical events and religious practices but also provide invaluable insights into the language,
042 society, and culture of early Chinese civilization, marking a pivotal stage in the evolution of Chinese
043 characters. Despite the discovery of approximately 4,500 OBS characters, only about 1,600 have
044 been successfully deciphered, leaving much of this ancient writing system still undeciphered.

045 During the decipherment of Oracle Bone Script (OBS), the most fundamental materials to re-
046 searchers are the approximately 150,000 excavated oracle bone fragments. However, these phys-
047 ical artifacts are dispersed across various locations, making it exceedingly difficult for schol-
048 ars to access the originals for in-depth study. To overcome this, scholars rely on rubbings,
049 which are paper impressions that capture the surface texture of the bones. As shown in Fig. 1,
050 these rubbings authentically preserve the original information of the oracle bones but often suf-
051 fer from unclear character shapes due to noise such as scratches. The corpus of rubbings cur-
052 rently amounts to about 200,000 pieces. Additionally, scholars produced facsimiles by manually
053 outlining the oracle bone characters. As illustrated in Fig. 1, these facsimiles feature clear char-
acter morphology but inevitably lose some details present on the original fragments. There are
approximately 70,000 such traced images that can be directly paired with corresponding rubbings.

054 Typically, research workflows of OBS involve comparing similar character forms,
 055 examining the interpretations of specific character across different rubbings, extracting
 056 comprehensive information from duplicate fragments, and synthesizing prior scholarship.
 057 However, the absence of Unicode encoding for OBS poses significant challenges for information retrieval. To address
 058 this, scholars compiled comprehensive reference works, such as *Oracle Bone Inscriptions Gulin* (Yu, 1996), *Oracle Bone Inscriptions Compendium* (Li, 2012), and *Yinxu Complete Collection of Facsimiles with Transcriptions of Oracle Bone Inscriptions* (Yao, 1998), which serve different purposes: aggregating philological interpretations, cataloging glyph variants, and providing collections of deciphered texts. Despite these efforts, the process has traditionally depended heavily on the expertise and memory of individual scholars. Conducting searches, comparisons, and syntheses across resources at the scale of 200K rubbings, reference works, and academic publications is both time-consuming and error-prone. For instance, even experienced experts may spend considerable time compiling evidence for a single character, while less experienced scholars may require significantly longer. Consequently, the efficiency and accuracy of information retrieval and organization have become critical bottlenecks in OBS research.

073 To address these challenges, we propose OracleAgent, the first agent system designed for the structured management and retrieval of OBS information. OracleAgent is capable of assisting researchers
 074 rapidly, accurately, and comprehensively in gathering relevant content and associated information.
 075 Our agent is meticulously designed around three core aspects: knowledge base construction, model-
 076 based toolchains, and task-oriented planning. This enables the agent to orchestrate tools according to
 077 the requirements of specific research tasks, leverage the knowledge base as an enhanced resource for
 078 retrieval and generation, and finally aggregate and synthesize all related information for researchers,
 079 thereby accelerating the decipherment process of Oracle Bone Script. Its architecture is carefully de-
 080 signed around three core components: **(1) Knowledge Bases:** From a content perspective, the data
 081 must comprehensively cover diverse aspects of OBS. We therefore construct five interlinked knowl-
 082 edge bases encompassing rubbings, facsimiles, single characters, interpretation texts, and scholarly
 083 literature. From a structural perspective, the heterogeneous combination of images and texts poses
 084 challenges for algorithmic processing. To mitigate this, we fragment and restructured resources
 085 such as 3,000 research papers and *Gulin* (Yu, 1996) to enable fine-grained retrieval. **(2) Domain**
 086 **Model-Driven Tools:** To enable precise and comprehensive retrieval from the knowledge bases, we
 087 develop a suite of algorithms, including single-character detection, glyph retrieval, rubbing retrieval,
 088 and facsimile generation. These algorithms not only enrich the knowledge bases through offline
 089 processing of raw data but also support online retrieval, ensuring that researchers can directly access the
 090 information relevant to their tasks. **(3) Task-Oriented Planning with LLMs:** Powered by LLMs,
 091 OracleAgent dynamically plans tasks based on the specific needs of researchers, autonomously se-
 092 lects and invokes the most suitable model-based tools for each subtask, and ultimately aggregates
 093 both retrieved and generated information into comprehensive, coherent outputs tailored to the user’s
 094 requirements.

095 The main contributions are summarized as: 1) We propose **OracleAgent**, the first AI agent sys-
 096 tem designed for the structured management and retrieval of OBS information, which seamlessly
 097 integrates seven OBS analysis tools, empowered by LLMs, dynamically orchestrating specialized
 098 components for complex OBS queries. 2) We propose the first comprehensive, domain-specific
 099 multimodal knowledge base for OBS, built through a rigorous multi-year process of data collec-
 100 tion, cleaning, and expert annotation. The knowledge base contains over **1.4M** single-character
 101 facsimile images and **80K** interpretation texts, supporting retrieval tasks of character, document,
 102 interpretation text, and rubbing image via the multiple tools integrated within OracleAgent. 3)
 103 OracleAgent provides comprehensive OBS analysis capabilities, including modality classification,
 104 character classification and retrieval, character detection, and facsimile generation. It dynamically
 105 orchestrates specialized tools based on user needs, retrieves information from knowledge bases, and
 106 synthesizes reliable results. 4) Extensive experiments demonstrate that OracleAgent outperforms
 107 leading MLLMs on OBS reasoning and generation tasks, while maintaining strong stability. Further
 case studies show that OracleAgent can effectively execute complex workflows and assist domain
 experts in retrieving relevant documents, significantly reducing the time required for OBS research.

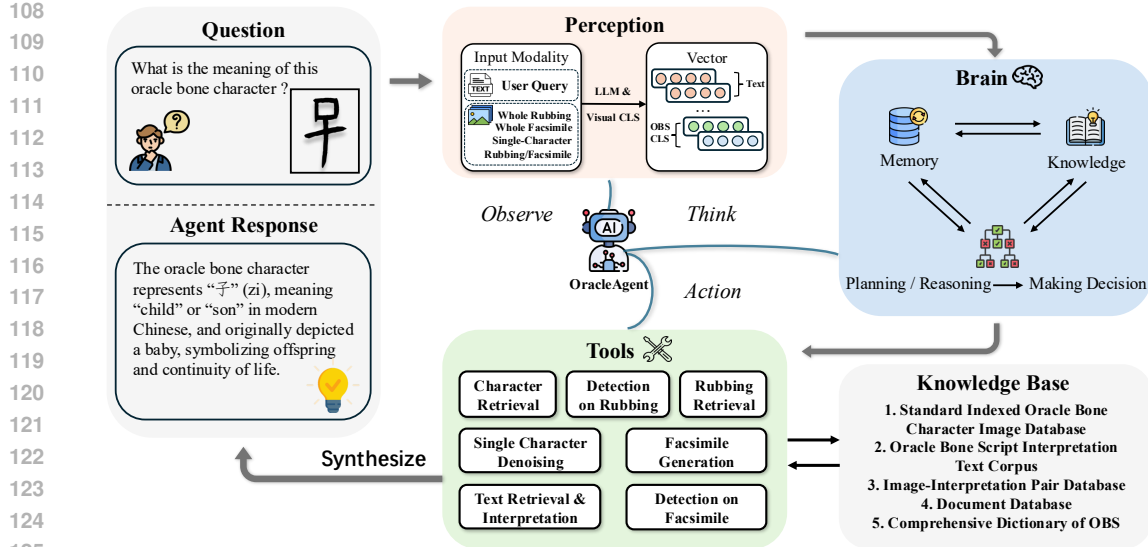


Figure 2: **Architecture overview of the proposed OracleAgent.** OracleAgent consists of four modules: Perception, Brain, Tools, and Knowledge Bases. The Perception module accepts multimodal user inputs and infers user intent. The Brain stores states in Memory and integrates multimodal reasoning with tool-based decision-making. Some tools integrated within OracleAgent are capable of retrieving information from knowledge base.

2 RELATED WORKS

Oracle Character Processing. Deep learning has played an important role in OBS processing. Recent studies (Jiang et al., 2023; Li et al., 2021; Wang et al., 2022; Gao et al., 2022) have focused on character detection, denoising, and image translation, while others, such as Genov (Qiao et al., 2024) and OracleFusion (Li et al., 2025b), leverage MLLMs to enhance visual understanding. More recently, OBS Decipher (OBSD) (Guan et al., 2024) has applied diffusion models to decipher oracle characters. Although these works are all centered on deep learning, their models are typically tailored to specific tasks and lack a unified framework capable of addressing the full range of OBS challenges. To bridge this gap, OBI-Bench (Chen et al., 2024b) introduces a comprehensive OBS benchmark for MLLMs, leveraging their strong prior knowledge to tackle various OBS tasks. However, due to issues such as hallucination and suboptimal performance of MLLMs on certain tasks, there remains a need for a more comprehensive, effective, and reliable AI system.

LLM-based Agent Architectures. Recent advances in LLM-powered agents have enabled autonomous reasoning, planning, and flexible tool utilization (Xi et al., 2025; Zhao et al., 2023; Matarman et al., 2024). Representative frameworks such as ReAct (Yao et al., 2023) combine reasoning and acting, while tool-calling methods (*e.g.*, Toolformer (Schick et al., 2023)) and multi-agent orchestration (*e.g.*, AutoGen (Wu et al., 2024)) further expand agent capabilities. However, their application in domain-specific tasks like OBS research is still underexplored, highlighting the need for customized agent frameworks incorporating domain knowledge and systematic tool coordination.

Evaluation Frameworks. A range of benchmarks have been developed to rigorously assess the capabilities of LLM-based agents. For example, AgentBench (Liu et al., 2023) evaluates agents on tasks such as multi-step reasoning, memory retention, tool utilization, task decomposition, and interactive problem solving. Findings indicate that even advanced models like GPT-4o and Claude-3.5-Sonnet face challenges with maintaining long-term context and making autonomous decisions. Building on these insights, MMAU (Yin et al., 2024) extends evaluation to five domains—tool use, graph reasoning, data science, programming, and mathematics—further exposing ongoing difficulties in structured reasoning and iterative problem solving. However, the evaluation of agents in the OBS domain remains unexplored. To address this gap, we compare our approach with general-purpose MLLMs and further extend the benchmark to the domain of facsimile generation.

162 3 ORACLEAGENT
163164 3.1 SYSTEM OVERVIEW
165

166 We present **OracleAgent**, a unified agent framework designed for various Oracle Bone Script (OBS)
167 tasks. Fig. 2 illustrates the workflow of our OracleAgent, which comprises four core modules: Per-
168 ception, Brain, Tools, and Knowledge Base. User queries are processed sequentially through these
169 modules, enabling adaptive and context-aware reasoning. The overall workflow is as follows: (1)
170 **Observe**: The Perception module ingests external inputs, including user queries and various types of
171 images, providing a comprehensive understanding of the environment. (2) **Think**: The Brain mod-
172 ule dynamically analyzes the current state maintained in Memory and performs structured reasoning
173 by orchestrating an array of specialized tools for decision-making. (3) **Action**: OracleAgent orches-
174 trates multiple tools in serial and parallel workflows to accomplish complex tasks. Furthermore, the
175 integrated multimodal tools within the agent leverage the domain-specific OBS knowledge base for
176 information retrieval, serve as a reliable source for retrieval- augmented generation.

177
178 3.2 KNOWLEDGE BASES
179

180 To better support OBS experts in the organization and study, we construct a comprehensive,
181 richly annotated image database of oracle bone characters together with a corresponding textual-
182 interpretation corpus. This resource is assembled through a multi-year effort involving extensive
183 manual collection, rigorous data cleaning, and meticulous annotation to maximize accuracy and
184 coverage. We further integrate a task-driven image-retrieval framework that leverages the image and
185 text retrieval tools described in Section 3.3. This framework matches input query images of oracle
186 bone characters to canonical forms stored in the database and then retrieves multiple candidate inter-
187 pretations from the textual corpus, thereby enabling automatic matching of isomorphic characters.
188 The knowledge base comprises five databases. In the first three databases, every image is annotated
189 with provenance information to ensure traceability. In addition, single-character entries, their tex-
190 tual interpretations, and their images are mutually cross-referencable via oracle bone fragment IDs.
191 Moreover, we curate a pixel-level fine-grained dataset of approximately 15K annotations that records
192 facsimile-rubbing correspondences, precise single-character locations, and explicit reading order,
providing a high-resolution foundation for downstream retrieval and analysis tasks.

- 193 • **Standard Indexed Oracle Bone Character Image Database** (Peichao, 2024): A meticulously
194 curated standard database of oracle bone characters, produced by domain experts, containing
195 50K images across 4,000 distinct characters and 6,000 subclasses. This database serves as the
196 reference for associating input character images with their standard forms.
- 197 • **Oracle Bone Script Interpretation Text Corpus**: A collection of interpretation texts for oracle
198 bone fragments, gathered from online sources, covering 60K fragments and 80K interpretation
199 texts. This corpus includes the meanings of characters, common phrases, and their occurrences in
200 various literature. The main sources include: (1) Oracle Bone Instructions (OBI) Collection (Guo
201 & Hu, 1978-1982), (2) Supplement to the OBI Collection (Peng et al., 1999) , (3) Huayuan East
202 Oracle Bones (Institute of Archaeology, 2003), and (4) Xiaotun South Oracle Bones (Liu, 1983).
- 203 • **Image-Interpretation Pair Database**: First, we apply the character-detection algorithm de-
204 scribed in Section 3.3 to a corpus of 172K rubbings from YinQiWenYuan (AYNU, 2020), yielding
205 1.4M cropped single-character images. To support efficient retrieval, we then generate facsimile
206 representations for each rubbing and each extracted character by applying the facsimile genera-
207 tion algorithm introduced in Section 3.3. Collectively, these processing steps produce the most
208 comprehensive database of image–interpretation pairs to date.
- 209 • **Document Database**: We construct our document database from the YiQinWenYuan, which pro-
210 vides richly interleaved image-text data on oracle bone studies. The database comprises 3,000
211 documents related to the interpretation of oracle bone characters, alongside three authoritative
212 reference books covering historical perspectives on specific characters. Text regions are extracted
213 from document images using PaddleOCR (Cui et al., 2025), and all character images are man-
214 ually segmented. Each image is indexed by its corresponding character, enabling precise image-text
215 alignment and facilitating efficient retrieval tasks in downstream modules.

216 • **Comprehensive Dictionary of OBS:** A database of interpretations for 7,000 oracle bone inscriptions, sourced from *Gulin* (Yu, 1996) and *Gulin Supplementary Volume* (He, 2017), with the same compilation methodology as the document database.

220 **3.3 DOMAIN MODEL TOOLS OF ORACLE BONE SCRIPT**

222 • **Character Detection on Rubbing.** We train a YOLO-based detection model on the rubbing image dataset to automatically localize oracle bone script (OBS) characters within rubbing images.

224 • **Character Detection on Facsimile.** We train a YOLO-based detection model on the facsimile image dataset to identify and extract oracle bone script (OBS) characters from facsimile images.

226 • **Text Retrieval and Interpretation.** We utilize the GTE-Qwen2-1.5B (Li et al., 2023) multi-
227 lingual embedding model instruction-tune on high-quality query–document pairs to retrieve and
228 interpret relevant textual information in response to user queries.

229 • **Character Retrieval and Classification.** To enable efficient character retrieval and classification
230 based on visual similarity, we train a feature extraction model (Ren et al., 2022) specifically
231 designed for characteristics of OBS facsimile images.

232 • **Single-Character Facsimile Image Denoising.** To transform noisy rubbing images of individual
233 OBS characters into clean facsimile representations, we employ and train a CycleGAN (Zhu et al.,
234 2017) model for this image-to-image translation task.

235 • **Whole Facsimile Image Generation.** To generate complete facsimile images from rubbing images.
236 We train a ControlNet (Zhang et al., 2023) based on SD1.5 (Rombach et al., 2022) on the
237 OBIMD dataset (Li et al., 2024) to achieve facsimile image generation.

238 • **Rubbing Image Retrieval.** We support efficient retrieval of rubbing images based on visual
239 similarity by training a specialized matching model (Li et al., 2025a). Furthermore, by leveraging
240 the Image-Interpretation Pair Database, the retrieved rubbing images can be indexed to their
241 corresponding interpretation texts, enabling effective rubbing-to-interpretation matching.

243 **3.4 OBS MULTIMODAL PERCEPTION AND BRAIN**

245 The Perception module constitutes the foundational component of our Oracle Bone Intelligent
246 Agent, enabling comprehensive understanding of both user queries and multiple visual modalities of
247 OBS. As illustrated in Fig. 1, The system processes a set of oracle bone images $I = \{I_1, \dots, I_i\}_{i=M}$
248 spanning modalities such as rubbings, facsimiles, single-character crops, and handprinted characters.
249 Each image I_i is encoded via a visual encoder \mathcal{V} to obtain modality-specific features:

$$\mathbf{v}_i = \mathcal{V}(I_i), i = 1, 2, \dots, M. \quad (1)$$

252 User queries Q are interpreted in the context of the visual inputs. Unlike conventional approaches
253 that combine multi-modal features via concatenation or attention mechanisms, our method employs
254 large language models (LLMs) by injecting discrete visual tokens into the textual prompt. Specifically,
255 visual features $\{\mathbf{v}_1, \mathbf{v}_2, \dots, \mathbf{v}_i\}_{i=M}$ are projected into tokens and embedded alongside the user
256 query to form a unified prompt, which can be formulated as:

$$Prompt = [Q; \mathbf{v}_1; \mathbf{v}_2; \dots; \mathbf{v}_i]_{i=M} \quad (2)$$

258 This unified prompt enables the Agent to jointly process textual and visual information, facilitating
259 deep semantic alignment and cross-modal reasoning through the LLM’s contextual capabilities.

260 The Brain module serves as the central reasoning and decision-making component of the Agent,
261 functioning as the “cognitive core” that orchestrates the overall workflow. Leveraging the powerful
262 prior knowledge embedded within large language models (LLMs), the Brain module is responsible
263 for analyzing the current state stored in Memory, planning tool usage, performing multi-step rea-
264 soning, and ultimately making decisions to fulfill user intents. At each interaction step, the Agent
265 maintains a dynamic state s_t in Memory, which encapsulates the historical context, user queries,
266 intermediate results, and relevant environmental information up to time t . The Brain module first
267 retrieves and interprets this state: $s_t = Memory(t)$. The state s_t is then encoded into a structured
268 prompt, which is fed into the LLM-based Brain for further analysis. Given the current state s_t , the
269 Brain module utilizes its extensive prior knowledge to plan the sequence of tool invocations required
to solve the task. Let $\mathcal{A} = \{a_1, a_2, \dots, a_j\}_{j=K}$ denote the set of available tools (e.g., *OCR*, *image*

270
 271 Table 1: Results on the OBS character retrieval task on OBC306 and OBI-IJDH datasets. “*Yes-or-*
 272 *No*” and “*How*” represent the absolute and probability output, respectively. We report the averaged
 273 Recall@1, 3, 5, and mAP@5 for “*How*” question.

274 275 276 277 278 279 280 281 282 283 284 285 286 287 288 289 290 291 292 293 294 295 296 297 298 299 300 301 302 303 304 305 306 307 308 309 310 311 312 313 314 315 316 317 318 319 320 321 322 323	OBC306			OBI-IJDH				
	275 276 277 278 279 280 281 282 283 284 285 286 287 288 289 290 291 292 293 294 295 296 297 298 299 300 301 302 303 304 305 306 307 308 309 310 311 312 313 314 315 316 317 318 319 320 321 322 323	275 276 277 278 279 280 281 282 283 284 285 286 287 288 289 290 291 292 293 294 295 296 297 298 299 300 301 302 303 304 305 306 307 308 309 310 311 312 313 314 315 316 317 318 319 320 321 322 323	275 276 277 278 279 280 281 282 283 284 285 286 287 288 289 290 291 292 293 294 295 296 297 298 299 300 301 302 303 304 305 306 307 308 309 310 311 312 313 314 315 316 317 318 319 320 321 322 323	275 276 277 278 279 280 281 282 283 284 285 286 287 288 289 290 291 292 293 294 295 296 297 298 299 300 301 302 303 304 305 306 307 308 309 310 311 312 313 314 315 316 317 318 319 320 321 322 323				
GPT-4v	0.4228	0.205	0.650	0.624	0.5680	0.225	0.676	0.740
GPT-4o	0.4550	0.235	0.686	0.688	0.6122	0.250	0.706	0.800
Qwen-VL-MAX	0.4223	0.190	0.621	0.644	0.5716	0.225	0.638	0.780
InternVL2-Llama3-76B	0.3557	0.150	0.460	0.522	0.4268	0.250	0.675	0.720
InternVL2-8B	0.2844	0.095	0.374	0.420	0.3623	0.225	0.650	0.68
Qwen-VL-7B	0.2883	0.080	0.345	0.422	0.3528	0.225	0.588	0.660
LLaVA-NeXT-8B	0.2793	0.075	0.358	0.348	0.3605	0.225	0.606	0.600
Qwen2.5-VL-7B	0.2995	0.110	0.388	0.460	0.3704	0.225	0.620	0.700
OracleAgent (Ours)	0.4953	0.210	0.690	0.712	0.7600	0.250	0.735	0.940

retrieval, translation, etc). At time t , the Brain constructs a plan π_t , which is an ordered sequence of tool actions: $\pi_t = [a_1, a_2, \dots, a_n]$, $a_i \in \mathcal{A}$, which maximizes the expected utility:

$$\pi_t = \arg \max_{\pi} \mathbb{E}[R(\pi \mid s_t, \text{Goal})], \quad (3)$$

where $R(\cdot)$ denotes the utility of executing plan π given the state s_t and the user goal.

4 ORACLEAGENT-BENCH

4.1 DATASET

For OBS detection, character classification, and character retrieval tasks, we use OBI-Bench (Chen et al., 2024b) to evaluate the understanding and reasoning ability of OracleAgent. Additionally, we introduce 3K images from 4 different OBS modalities illustrated in Fig. 1 to evaluate the OBS modality classification and facsimile generation ability.

4.2 QUESTION SETTINGS

To evaluate various perception capabilities, we follow the coarse-to-fine question settings in OBI-Bench. Specifically, we categorize the questions into four distinct types: (1) **Yes-or-No**: Binary questions designed to minimize ambiguity and directly reflect the underlying task objectives. (2) **Which**: Single-choice questions that require the model to identify the correct answer from a finite set of candidates, thereby evaluating its discriminative capability among closely related options. (3) **How**: Quantitative questions, such as determining the number of oracle bone characters present in an image or estimating the probability that two characters belong to the same class, which facilitate a more fine-grained assessment of model performance. (4) **Where**: Localization questions that prompt the model to output bounding boxes for detected characters, thereby assessing its spatial reasoning and detailed perceptual abilities. For facsimile generation task, we prompt the model with instruction: “Please transform this picture into a facsimile.”.

5 EXPERIMENTS

5.1 IMPLEMENTATIONS

OracleAgent employs DeepSeek-V3.1 (Liu et al., 2024a) as its backbone LLM and integrates Yolov11 (Khanam & Hussain, 2024) for character detection, GTE-Qwen2-1.5B (Li et al., 2023)

Table 2: Results on the OBS detection task. “*How*” and “*Where*” represent the number and bounding box output, respectively. We report MRE and mIoU.

295 296 297 298 299 300 301 302 303 304 305 306 307 308 309 310 311 312 313 314 315 316 317 318 319 320 321 322 323	295 296 297 298 299 300 301 302 303 304 305 306 307 308 309 310 311 312 313 314 315 316 317 318 319 320 321 322 323	295 296 297 298 299 300 301 302 303 304 305 306 307 308 309 310 311 312 313 314 315 316 317 318 319 320 321 322 323	295 296 297 298 299 300 301 302 303 304 305 306 307 308 309 310 311 312 313 314 315 316 317 318 319 320 321 322 323	
GPT-4v		Closed	0.4383	0.0165
GPT-4o		Closed	0.3458	0.0182
Qwen-VL-MAX		Closed	0.4843	0.0131
InternVL2-Llama3-76B		Open	0.5344	0.0623
InternVL2-8B		Open	1.1146	0.0152
Qwen-VL-7B		Open	3.5694	0.0069
LLaVA-NeXT-8B		Open	0.4268	0.0189
Qwen2.5-VL-7B		Open	1.0000	<u>0.1112</u>
OracleAgent (Ours)		Open	0.3894	0.6198

324
325
326
327
328
329
330
331
332
333
334
335
336
337
338
339
340
341
342
343
344
345
346
347
348
349
350
351
352
353
354
355
356
357
358
359
360
361
362
363
364
365
366
367
368
369
370
371
372
373
374
375
376
377
Table 3: Results on the OBS character classification task on HWOBC, Oracle50K, and OBI125 datasets. Note that “*Yes-or-No*” and “*How*” represent absolute and probability output, respectively.

Models	HWOBC			Oracle-50k			OBI125		
	<i>Yes-or-No</i> ↑		<i>How</i> ↑	<i>Yes-or-No</i> ↑		<i>How</i> ↑	<i>Yes-or-No</i> ↑		<i>How</i> ↑
	Acc	Acc@1	Acc@5	Acc	Acc@1	Acc@5	Acc	Acc@1	Acc@5
GPT-4v	69.50	86.75	100.0	66.00	88.25	100.0	57.75	70.75	91.75
GPT-4o	<u>72.75</u>	<u>89.75</u>	100.0	<u>74.50</u>	<u>90.25</u>	100.0	<u>62.50</u>	<u>75.50</u>	<u>93.75</u>
Qwen-VL-MAX	64.25	85.00	100.0	65.75	88.75	98.75	55.00	69.25	89.75
InternVL2-Llama3-76B	44.75	53.75	69.75	47.50	55.00	69.00	43.25	50.75	66.75
Qwen-VL-7B	44.25	48.00	61.25	42.00	51.00	63.50	38.75	44.75	61.25
InternVL2-8B	42.25	47.75	59.75	41.75	49.00	59.00	38.75	47.75	56.50
LLaVA-NeXT-8B	44.00	46.75	53.75	42.00	46.25	56.75	38.75	42.75	54.75
Qwen2.5-VL-7B	45.50	49.25	65.25	43.25	51.75	65.25	42.50	47.25	62.75
OracleAgent (Ours)	89.75	95.75	100.0	90.25	92.75	100	80.50	84.75	95.00

for text retrieval and interpretation, EGFF model (Ren et al., 2022) for Glyph Retrieval and Classification, CycleGAN (Zhu et al., 2017) and ControlNet (Zhang et al., 2023) for facsimile generation. OracleAgent executes tool operations via structured JSON API calls, explicitly specifying all required parameters (*e.g.*, *image file locations*, *textual instructions*) for each target tool. For baseline comparisons, we use the official implementations of all models and strictly follow their recommended configuration protocols during evaluation. For model responses, we employ regular expressions to extract answers such as numerical values or boolean results. In cases of errors or timeouts, the extraction procedure is retried up to three times. If the response remains invalid or does not yield a single definitive answer after these attempts, it is marked as incorrect.

5.2 EXPERIMENTAL SETUP

We evaluate OracleAgent against both mainstream open-source and proprietary MLLMs, including the Qwen (Bai et al., 2023), GPT-4 (Hurst et al., 2024), InternVL (Chen et al., 2024a), and LLaVA (Liu et al., 2024b) series. Since most MLLMs lack the advanced instruction-based image editing capabilities like GPT-4o, we additionally compare OracleAgent with Bagel (Deng et al., 2025) and Step1x-Edit (Liu et al., 2025) on the facsimile generation task. We conduct comprehensive evaluations on OracleAgent-Bench, which incorporates experimental settings from OBI-Bench for oracle bone script (OBS) detection, character classification, and retrieval tasks. For modality classification and generation tasks, we design tailored evaluation procedures and metrics. The experimental configurations for the five key domain problems are detailed as follows:

Character Retrieval and Classification. To evaluate model performance on oracle bone character retrieval and classification tasks, we design “*Yes-or-No*” and “*How*” questions. Specifically, these questions are constructed based on intra-class and inter-class pairs of oracle bone character images, requiring the model to output either a binary decision or a probabilistic score indicating class similarity. The retrieval task includes 600 images sampled from OBC306 (Huang et al., 2019) and OBI-IJDH (Fujikawa & Meng, 2020). We employ averaged Recall@k and mean Average Precision (mAP) to quantify the multi-round OBI retrieval performance of MLLMs and OracleAgent. The character classification task comprises 500 images across 100 categories from each of HWOBC (Li et al., 2020), Oracle-50k (Han et al., 2020), and OBI125 (Yue et al., 2022), with accuracy (Acc) used as the evaluation metric.

Detection. To assess model performance on OBS detection, we employ two question types to evaluate coarse- and fine-grained perceptual abilities with 2K OBS rubbing images sampled from YinQi-WenYuan (AYNU, 2020). “*How*” questions require the model to predict the number of characters on a given rubbing, while “*Where*” questions task the model with precisely localizing each character by outputting its bounding box. We utilize MRE described in Eq. 4 and mIoU

Modality Classification. We utilize 2K images from OBIMD (Li et al., 2024), covering four distinct OBS image modalities. For each image, we present a “*Which*” question, requiring the model to select the most appropriate modality from four given options.

Generation. The facsimile generation task converts oracle bone rubbing images into corresponding facsimiles via a simple prompt (*e.g.*, “*Please convert this to a facsimile.*”). Most existing MLLMs lack the instruction-driven image editing capabilities of models like GPT-4o. We evaluate OracleAgent against unified autoregressive models, including Bagel (Deng et al., 2025), Flux1.-

378 Kontext (Batifol et al., 2025), and Step1x-Edit (Liu et al., 2025). We sample 500 rubbing-facsimile
 379 pairs from designated test set of the OBIMD dataset and assess performance using standard met-
 380 rics: FID (Heusel et al., 2017), KID (Bińkowski et al., 2018), SSIM (Wang et al., 2004), and
 381 LPIPS (Zhang et al., 2018). For further details, please refer to the OBI-Bench paper (Chen et al.,
 382 2024b) and Appendix E of our work.

383 **Case Study of Retrieval Evaluation.** For the retrieval task of a specific oracle character, we use
 384 expert-annotated results as the ground truth and compare them with the retrieval results obtained by
 385 OracleAgent. Specifically, we evaluate the retrieval performance using Precision, Recall, F1-score,
 386 and Coverage, with their respective definitions and calculation formulas provided in Eq. 5-Eq. 8.
 387

388 390 5.3 QUANTITATIVE ANALYSIS

391 **Retrieval.** As shown in Tab. 1, all
 392 models exhibit comparable performance
 393 on the character retrieval task under
 394 the Recall@1 metric, with OracleAgent
 395 slightly trailing GPT-4o on the OBC306
 396 dataset. However, when expanding the
 397 candidate pool to Recall@3 and Re-
 398 call@5, OracleAgent consistently out-
 399 performs all baselines on both the
 400 OBC306 and OBI-IJDH datasets across
 401 “Yes-or-No” and “How” question types.
 402 This indicates that OracleAgent is more
 403 effective at retrieving relevant characters when a broader set of candidates is considered, which is
 404 critical for practical applications. These findings also underscore the limitations of Recall@1 in
 405 distinguishing model capabilities. Moreover, OracleAgent achieves the highest mAP@5 scores on
 406 both datasets, further demonstrating its superior retrieval performance and robustness in complex
 407 character retrieval scenarios compared to state-of-the-art models.

408 **Character Classification.** Tab. 3 presents OBS character classification results on HWOB, Oracle-
 409 50k, and OBI125. OracleAgent consistently achieves the highest accuracy on both “Yes-or-No” and
 410 “How” questions across all datasets. While proprietary models such as Qwen and GPT-4 outperform
 411 open-source MLLMs, OracleAgent maintains a clear lead, particularly in Acc@5. These results
 412 demonstrate its superior classification and generalization capabilities.

413 **Detection.** As shown in Tab. 2, OracleAgent achieves the highest performance on the “Where”
 414 (mIoU) metric with a score of 0.6198, significantly outperforming all baselines and demonstrating
 415 strong localization capability. On the “How” (MRE) metric, OracleAgent attains 0.3894, slightly
 416 higher than GPT-4o but better than most open models, indicating robust numerical prediction. Over-
 417 all, OracleAgent substantially improves target localization accuracy while maintaining low quantity
 418 prediction error, highlighting its superior fine-grained perception.

419 **Modality Classification.** As shown in Tab. 4, OracleAgent achieves an accuracy of 99.9% on
 420 the modality classification task. Since modality classification is a fundamental step upon which
 421 subsequent workflows depend, such high accuracy is crucial. Moreover, other models lack access to
 422 multimodal OBS training data, which reasonably accounts for their lower zero-shot performance.

423 **Evaluation on Generation** As shown
 424 in Tab. 5, OracleAgent outperforms all
 425 baselines on the OBS facsimile gen-
 426 eration task across all evaluation met-
 427 rics. OracleAgent produces facsimiles
 428 that are both visually and perceptually
 429 closer to the ground truth, with FID and
 430 KID reduced by more than half com-
 431 pared to GPT-4o, and notable gains in SSIM and LPIPS. These results highlight OracleAgent’s
 432 advanced fine-grained facsimile image generation capability.

388 390 Table 4: Results on the OBS modality classification task.

Models	Type	Which↑		
		Acc@1	Precision	Recall
Qwen-VL-MAX	Closed	83.35	0.8731	0.8345
Qwen-VL-PLUS	Closed	70.40	0.8561	0.7050
InternVL2-8B	Open	65.95	0.7748	0.6595
Qwen-VL-7B	Open	35.45	0.3734	0.2665
LLaVA-NeXT-8B	Open	39.55	0.4465	0.2955
Qwen2.5-VL-7B	Open	43.75	0.5434	0.4375
OracleAgent (Ours)	Open	99.90	0.9990	0.9975

423 Table 5: Results on the OBS facsimile generation task.

Models	FID↓	KID↓	SSIM↑	LPIPS↓
GPT-4o	103.65	68.19	0.8127	0.2787
Step1x-Edit	303.93	292.56	0.5876	0.4853
Flux.1-Kontext	225.88	196.73	0.7232	0.3491
Bagel-7B	144.02	95.97	0.7087	0.3417
OracleAgent (Ours)	45.06	24.00	0.8381	0.2447

432 5.4 CASE STUDY
433434 5.4.1 INTERACTION FLOW
435

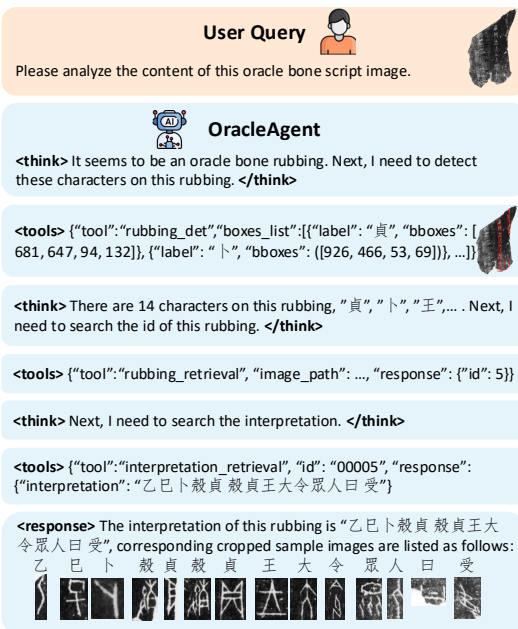
436 As shown in Fig. 3, the user’s question con-
437 cerns the analysis of a given oracle bone rub-
438 bing. OracleAgent first recognizes the modal-
439 ity of the OBS rubbing image. Next, it auto-
440 matically invokes the object detection tool
441 to accurately identify all oracle bone char-
442 acters present on the rubbing. Using the rub-
443 bing retrieval tool, it then determines the frag-
444 ment number, thereby obtaining the correct
445 reading order of the characters. Finally, by
446 calling the interpretation retrieval tool, Orac-
447 leAgent retrieves the corresponding modern
448 Chinese characters and aligns each oracle bone
449 character with its modern counterpart. This
450 process simulates the workflow of OBS ex-
451 pert and can greatly simplify their work. The
452 subsequent interaction is displayed in Fig. 4.

453 5.4.2 RETRIEVAL EVALUATION
454

455 To comprehensively assess the performance
456 of OracleAgent in real-world OBS infor-
457 mation retrieval tasks, we conducted a compara-
458 tive experiment against domain experts’ manual
459 search results. Specifically, we selected a target
460 oracle character and tasked both OracleAgent
461 and human experts with identifying all oracle
462 bone fragments in which the character appears.
463 For the expert baseline, a team of domain spe-
464 cialists engaged in manual retrieval by consulting
465 relevant reference books and materials over a one-week
466 period. The aggregated expert findings serve as the ground truth (noting that these results might
467 not be fully exhaustive, but currently represent the best available benchmark). OracleAgent sub-
468 sequently performed the same retrieval task automatically, and its results were directly compared
469 with those from the experts. As shown in Tab. 6, OracleAgent demonstrated strong performance on
470 this task, achieving a high recall of 92.69% and category coverage of 96.15%. These metrics indi-
471 cate a high level of agreement between OracleAgent and expert results. Additionally, OracleAgent
472 retrieved 7.31% more potential instances than the experts, with the majority of these additional find-
473 ings validated as reasonable upon further expert review. This highlights OracleAgent’s expert-level
474 retrieval capabilities and its potential to outperform manual expert searches, thus providing a robust
475 foundation for accelerating information retrieval and research in oracle bone studies.

476 6 CONCLUSION
477

478 In this work, we introduce OracleAgent, a pione-
479 ering AI agent system for the structured man-
480 agement and retrieval of OBS information. OracleAgent addresses two long-standing challenges in
481 OBS research: the complexity of interpretation workflows and inefficiencies in information organi-
482 zation and retrieval. By seamlessly integrating multiple OBS model-driven tools via large language
483 models (LLMs) and orchestrating them flexibly, OracleAgent enables end-to-end support for expert
484 tasks. Our comprehensive OBS multimodal knowledge base, comprising over 1.4 million char-
485 acter rubbing images and 80K interpretation texts, substantially enhances the system’s capabilities.
486 Experimental results and case studies demonstrate that OracleAgent achieves state-of-the-art per-
487 formance and significantly reduces the time required for OBS research. Our findings underscore
488 OracleAgent as an important advance toward intelligent, automated support in OBS research. Look-
489 ing ahead, we plan to further expand the coverage of the knowledge base and explore adaptive agent
490 strategies for broader semiotic and historical domains. We anticipate that OracleAgent will serve as
491 a foundation for future progress in computational humanities and the digitization of ancient scripts.



486 7 REPRODUCIBILITY STATEMENT
487488 We have already elaborated on all the models or algorithms proposed, experimental configurations,
489 and benchmarks used in the experiments in the main body or appendix of this paper. Furthermore,
490 we declare that the entire code used in this work will be released after acceptance.
491492 REFERENCES
493494 AYNU. Yinqiwenyuan: Oracle bone character detection dataset. <https://jgw.aynu.edu.cn/home/down/detail/index.html?sysid=3>, 2020. 2020.495 Jinze Bai, Shuai Bai, Shusheng Yang, Shijie Wang, Sinan Tan, Peng Wang, Junyang Lin, Chang
496 Zhou, and Jingren Zhou. Qwen-vl: A versatile vision-language model for understanding, local-
497 ization, text reading, and beyond, 2023. URL <https://arxiv.org/abs/2308.12966>.
498500 Stephen Batifol, Andreas Blattmann, Frederic Boesel, Saksham Consul, Cyril Diagne, Tim Dock-
501 horn, Jack English, Zion English, Patrick Esser, Sumith Kulal, et al. Flux. 1 kontext: Flow match-
502 ing for in-context image generation and editing in latent space. *arXiv e-prints*, pp. arXiv–2506,
503 2025.504 Mikołaj Bińkowski, Danica J Sutherland, Michael Arbel, and Arthur Gretton. Demystifying mmd
505 gans. *arXiv preprint arXiv:1801.01401*, 2018.
506507 Zhe Chen, Jiannan Wu, Wenhui Wang, Weijie Su, Guo Chen, Sen Xing, Muyan Zhong, Qinglong
508 Zhang, Xizhou Zhu, Lewei Lu, et al. Internvl: Scaling up vision foundation models and aligning
509 for generic visual-linguistic tasks. In *Proceedings of the IEEE/CVF conference on computer*
510 *vision and pattern recognition*, pp. 24185–24198, 2024a.511 Zijian Chen, Tingzhu Chen, Wenjun Zhang, and Guangtao Zhai. Obi-bench: Can Imms aid in study
512 of ancient script on oracle bones? *arXiv preprint arXiv:2412.01175*, 2024b.
513514 Cheng Cui, Ting Sun, Manhui Lin, Tingquan Gao, Yubo Zhang, Jiaxuan Liu, Xueqing Wang, Zelun
515 Zhang, Changda Zhou, Hongen Liu, Yue Zhang, Wenyu Lv, Kui Huang, Yichao Zhang, Jing
516 Zhang, Jun Zhang, Yi Liu, Dianhai Yu, and Yanjun Ma. Paddleocr 3.0 technical report, 2025.
517 URL <https://arxiv.org/abs/2507.05595>.518 Chaorui Deng, Deyao Zhu, Kunchang Li, Chenhui Gou, Feng Li, Zeyu Wang, Shu Zhong, Weihao
519 Yu, Xiaonan Nie, Ziang Song, et al. Emerging properties in unified multimodal pretraining. *arXiv*
520 *preprint arXiv:2505.14683*, 2025.521 Yoshiyuki Fujikawa and Lin Meng. Obi dataset for ijdh and obi recognition application. <http://www.ihpc.se.ritsumei.ac.jp/OBIdataeIJDH.zip>, 2020. 2020.522 Feng Gao, Jingping Zhang, Yong ge Liu, and Yahong Han. Image translation for oracle bone char-
523 acter interpretation. *Symmetry*, 14:743, 2022. URL <https://api.semanticscholar.org/CorpusID:247959908>.
524525 Haisu Guan, Huanxin Yang, Xinyu Wang, Shengwei Han, Yongge Liu, Lianwen Jin, Xiang Bai, and
526 Yuliang Liu. Deciphering oracle bone language with diffusion models. In Lun-Wei Ku, Andre
527 Martins, and Vivek Srikumar (eds.), *Proceedings of the 62nd Annual Meeting of the Association*
528 *for Computational Linguistics (Volume 1: Long Papers)*, pp. 15554–15567, Bangkok, Thailand,
529 August 2024. Association for Computational Linguistics. doi: 10.18653/v1/2024.acl-long.831.
530 URL <https://aclanthology.org/2024.acl-long.831>.
531532 Moruo Guo and Houxuan Hu. *Collection of Oracle Bone Inscriptions*. Zhonghua Book Company,
533 Beijing, China, 1978-1982.
534535 Wenhui Han, Xinlin Ren, Hangyu Lin, Yanwei Fu, and Xiangyang Xue. Self-supervised learning
536 of orc-bert augmentator for recognizing few-shot oracle characters. In *Proceedings of the Asian*
537 *Conference on Computer Vision*, 2020.538 Jingcheng He. Zhonghua Book Company, Beijing, China, 2017.
539

540 Martin Heusel, Hubert Ramsauer, Thomas Unterthiner, Bernhard Nessler, and Sepp Hochreiter.
 541 Gans trained by a two time-scale update rule converge to a local nash equilibrium. *Advances in*
 542 *neural information processing systems*, 30, 2017.

543

544 Shuangping Huang, Haobin Wang, Yongge Liu, Xiaosong Shi, and Lianwen Jin. Obc306: A large-
 545 scale oracle bone character recognition dataset. In *2019 International Conference on Document*
 546 *Analysis and Recognition (ICDAR)*, pp. 681–688. IEEE, 2019.

547

548 Aaron Hurst, Adam Lerer, Adam P Goucher, Adam Perelman, Aditya Ramesh, Aidan Clark, AJ Os-
 549 trow, Akila Welihinda, Alan Hayes, Alec Radford, et al. Gpt-4o system card. *arXiv preprint*
 550 *arXiv:2410.21276*, 2024.

551

552 Chinese Academy of Social Sciences Institute of Archaeology. *Oracle Bones from the Eastern*
 553 *Huayuanzhuang Site at Yin Xu*. Yunnan People’s Publishing House, Kunming, China, 2003.

554

555 Runhua Jiang, Yongge Liu, Boyuan Zhang, Xu Chen, Deng Li, and Yahong Han. Oraclepoints: A
 556 hybrid neural representation for oracle character. In *Proceedings of the 31st ACM International*
 557 *Conference on Multimedia*, MM ’23, pp. 7901–7911, New York, NY, USA, 2023. Association for
 558 Computing Machinery. ISBN 9798400701085. doi: 10.1145/3581783.3612534. URL <https://doi.org/10.1145/3581783.3612534>.

559

560 Rahima Khanam and Muhammad Hussain. Yolov11: An overview of the key architectural enhance-
 561 ments. *arXiv preprint arXiv:2410.17725*, 2024.

562

563 Bang Li, Qianwen Dai, Feng Gao, Weiye Zhu, Qiang Li, and Yongge Liu. Hwobc-a handwriting
 564 oracle bone character recognition database. In *Journal of Physics: Conference Series*, volume
 1651, pp. 012050. IOP Publishing, 2020.

565

566 Bang Li, Donghao Luo, Yujie Liang, Jing Yang, Zengmao Ding, Xu Peng, Boyuan Jiang, Shengwei
 567 Han, Dan Sui, Peichao Qin, et al. Oracle bone inscriptions multi-modal dataset. *arXiv preprint*
 568 *arXiv:2407.03900*, 2024.

569

570 Bang Li, Zengmao Ding, Yan Zhang, Han Zhang, Jing Yang, Jiaqi Fang, Taisong Jin, Yongge Liu,
 571 Zhenhao Song, and Rongrong Ji. An open benchmark for oracle bone rubbing image retrieval.
npj Heritage Science, 13(1):292, 2025a.

572

573 Caoshuo Li, Zengmao Ding, Xiaobin Hu, Bang Li, Donghao Luo, AndyPian Wu, Chaoyang
 574 Wang, Chengjie Wang, Taisong Jin, Yunsheng Wu, et al. Oraclefusion: Assisting the decipher-
 575 ment of oracle bone script with structurally constrained semantic typography. *arXiv preprint*
 576 *arXiv:2506.21101*, 2025b.

577

578 Jing Li, Qiu-Feng Wang, Rui Zhang, and Kaizhu Huang. Mix-up augmentation for oracle char-
 579 acter recognition with imbalanced data distribution. In *Document Analysis and Recognition –*
580 ICDAR 2021: 16th International Conference, Lausanne, Switzerland, September 5–10, 2021,
581 Proceedings, Part I, pp. 237–251, Berlin, Heidelberg, 2021. Springer-Verlag. ISBN 978-3-
 030-86548-1. doi: 10.1007/978-3-030-86549-8_16. URL https://doi.org/10.1007/978-3-030-86549-8_16.

582

583 Zehan Li, Xin Zhang, Yanzhao Zhang, Dingkun Long, Pengjun Xie, and Meishan Zhang. Towards
 584 general text embeddings with multi-stage contrastive learning. *arXiv preprint arXiv:2308.03281*,
 585 2023.

586

587 Zongkun Li. *Oracle Bone Inscriptions Compendium*. Zhonghua Book Company, Beijing, China,
 588 2012.

589

590 Aixin Liu, Bei Feng, Bing Xue, Bingxuan Wang, Bochao Wu, Chengda Lu, Chenggang Zhao,
 591 Chengqi Deng, Chenyu Zhang, Chong Ruan, et al. DeepSeek-V3 technical report. *arXiv preprint*
 592 *arXiv:2412.19437*, 2024a.

593

Haotian Liu, Chunyuan Li, Yuheng Li, Bo Li, Yuanhan Zhang, Sheng Shen, and Yong Jae Lee.
 Llavanext: Improved reasoning, ocr, and world knowledge, 2024b.

594 Shiyu Liu, Yucheng Han, Peng Xing, Fukun Yin, Rui Wang, Wei Cheng, Jiaqi Liao, Yingming
 595 Wang, Honghao Fu, Chunrui Han, et al. Step1x-edit: A practical framework for general image
 596 editing. *arXiv preprint arXiv:2504.17761*, 2025.

597

598 Xiao Liu, Hao Yu, Hanchen Zhang, Yifan Xu, Xuanyu Lei, Hanyu Lai, Yu Gu, Hangliang Ding,
 599 Kaiwen Men, Kejuan Yang, et al. Agentbench: Evaluating llms as agents. *arXiv preprint*
 600 *arXiv:2308.03688*, 2023.

601 Yiman Liu. *Oracle Bones from the Southern Xiaotun Site*. Zhonghua Book Company, Beijing,
 602 China, 1983.

603

604 Tula Masterman, Sandi Besen, Mason Sawtell, and Alex Chao. The landscape of emerging
 605 ai agent architectures for reasoning, planning, and tool calling: A survey. *arXiv preprint*
 606 *arXiv:2404.11584*, 2024.

607 Qin Peichao. Jingyuan oracle bone font library. <https://oracular.azurewebsites.net/>, 2024. 2024.

608

609 Bangjiong Peng, Ji Xie, and Jifan Ma. *Supplementary Collection of Oracle Bone Inscriptions*.
 610 Chinese Language and Literature Publishing House, Beijing, China, 1999.

611

612 Runqi Qiao, Lan Yang, Kaiyue Pang, and Honggang Zhang. Making visual sense of oracle bones
 613 for you and me. *CVPR*, Jan 2024.

614

615 Hao Ren, Ziqiang Zheng, and Hong Lu. Energy-guided feature fusion for zero-shot sketch-based
 616 image retrieval. *Neural Processing Letters*, 54(6):5711–5720, 2022.

617

618 Robin Rombach, Andreas Blattmann, Dominik Lorenz, Patrick Esser, and Björn Ommer. High-
 619 resolution image synthesis with latent diffusion models. In *Proceedings of the IEEE/CVF confer-
 620 ence on computer vision and pattern recognition*, pp. 10684–10695, 2022.

621

622 Timo Schick, Jane Dwivedi-Yu, Roberto Dessì, Roberta Raileanu, Maria Lomeli, Luke Zettlemoyer,
 623 Nicola Cancedda, and Thomas Scialom. Toolformer: Language models can teach themselves to
 624 use tools, 2023. *arXiv preprint arXiv:2302.04761*, 2023.

625

626 Mei Wang, Weihong Deng, and Cheng-Lin Liu. Unsupervised structure-texture separation network
 627 for oracle character recognition. *IEEE Transactions on Image Processing*, 31:3137–3150, 2022.
 doi: 10.1109/TIP.2022.3165989.

628

629 Zhou Wang, Alan C Bovik, Hamid R Sheikh, and Eero P Simoncelli. Image quality assessment:
 630 from error visibility to structural similarity. *IEEE transactions on image processing*, 13(4):600–
 612, 2004.

631

632 Qingyun Wu, Gagan Bansal, Jieyu Zhang, Yiran Wu, Beibin Li, Erkang Zhu, Li Jiang, Xiaoyun
 633 Zhang, Shaokun Zhang, Jiale Liu, et al. Autogen: Enabling next-gen llm applications via multi-
 634 agent conversations. In *First Conference on Language Modeling*, 2024.

635

636 Zhiheng Xi, Wenxiang Chen, Xin Guo, Wei He, Yiwen Ding, Boyang Hong, Ming Zhang, Junzhe
 637 Wang, Senjie Jin, Enyu Zhou, et al. The rise and potential of large language model based agents:
 638 A survey. *Science China Information Sciences*, 68(2):121101, 2025.

639

640 Shunyu Yao, Jeffrey Zhao, Dian Yu, Nan Du, Izhak Shafran, Karthik Narasimhan, and Yuan Cao.
 641 React: Synergizing reasoning and acting in language models. In *International Conference on
 642 Learning Representations (ICLR)*, 2023.

643

644 Xiaosui Yao. *Yinxu Complete Collection of Facsimiles with Transcriptions of Oracle Bone Inscript-
 645 tions*. Zhonghua Book Company, Beijing, China, 1998.

646

647 Guoli Yin, Haoping Bai, Shuang Ma, Feng Nan, Yanchao Sun, Zhaoyang Xu, Shen Ma, Jiarui Lu,
 648 Xiang Kong, Aonan Zhang, et al. Mmau: A holistic benchmark of agent capabilities across
 649 diverse domains. *arXiv preprint arXiv:2407.18961*, 2024.

650

651 Shengwu Yu. *Oracle Bone Inscriptions Gulin*. Zhonghua Book Company, Beijing, China, 1996.

648 Xuebin Yue, Hengyi Li, Yoshiyuki Fujikawa, and Lin Meng. Dynamic dataset augmentation for deep
 649 learning-based oracle bone inscriptions recognition. *ACM Journal on Computing and Cultural
 650 Heritage*, 15(4):1–20, 2022.

651 Lvmi Zhang, Anyi Rao, and Maneesh Agrawala. Adding conditional control to text-to-image
 652 diffusion models. In *Proceedings of the IEEE/CVF international conference on computer vision*,
 653 pp. 3836–3847, 2023.

654 Richard Zhang, Phillip Isola, Alexei A Efros, Eli Shechtman, and Oliver Wang. The unreasonable
 655 effectiveness of deep features as a perceptual metric. In *Proceedings of the IEEE conference on
 656 computer vision and pattern recognition*, pp. 586–595, 2018.

657 Pengyu Zhao, Zijian Jin, and Ning Cheng. An in-depth survey of large language model-based
 658 artificial intelligence agents. *arXiv preprint arXiv:2309.14365*, 2023.

659 Jun-Yan Zhu, Taesung Park, Phillip Isola, and Alexei A Efros. Unpaired image-to-image translation
 660 using cycle-consistent adversarial networks. In *Proceedings of the IEEE international conference
 661 on computer vision*, pp. 2223–2232, 2017.

662

663 A APPENDIX

664

665 B THE USE OF LARGE LANGUAGE MODELS

666

667 We use large language models solely for polishing our writing, and we have conducted a careful
 668 check, taking full responsibility for all content in this work.

669

670 C ETHICS STATEMENT

671

672 In alignment with the ICLR Code of Ethics, our work centers on publicly available, open-licensed
 673 images of oracle bone script. No sensitive, private, or personally identifiable information has been
 674 incorporated at any stage of dataset development or annotation. We exercised particular care to re-
 675 spect cultural heritage and maintain fairness throughout the entire process. To promote transparency
 676 and replicability within oracle bone script research, we commit to sharing our dataset and algo-
 677 rithmic resources for academic use only. By doing so, we hope to advance responsible research
 678 practices and contribute positively to the scholarly study of ancient scripts.

679

680 D ADDITIONAL CASE STUDY

681

682 In Section 5.4 of the main paper, we present
 683 only a portion of the results from our case study.
 684 The subsequent user query. In the subsequent
 685 interaction, the user follows up on the previ-
 686 ous response by inquiring about a specific or-
 687 acle bone character identified in the initial anal-
 688 ysis in Fig. 4. This scenario reflects a typi-
 689 cal expert workflow, where further investiga-
 690 tion is required for a particular character of
 691 interest. OracleAgent recognizes that the query per-
 692 tains to a single character cropped from an
 693 oracle bone rubbing. Given that our Standard
 694 Index Database is organized by facsimile modal-
 695 ity, OracleAgent first performs single-character
 696 denoising to generate the facsimile form of the
 697 queried character. It then utilizes the character
 698 retrieval tool to locate the standard glyph within
 699 the index database and further retrieves visually
 700 similar glyphs from the Image-Interpretation
 701

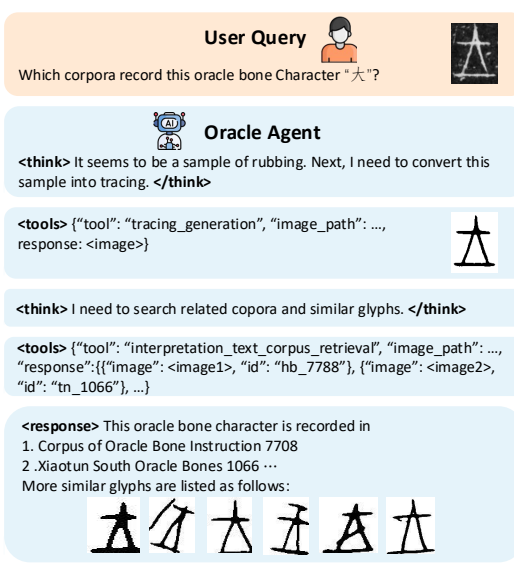


Figure 4: **OracleAgent Interaction Flow:**
 Follow-up query about which catalogues record
 this oracle bone character from the last response.

702 Pair Database, linking each to the corresponding
 703 interpretation and corpus.
 704

705 E DETAILED EXPERIMENTAL CONFIGURATION

708 In this section, we provide a comprehensive description of the experimental setup, including a diverse set of OBS tasks. Specifically, we exhibit the question templates of different oracle bone script
 709 tasks.
 710

712 E.1 CHARACTER RETRIEVAL AND CLASSIFICATION

714 “How” question template:

715 *#System: You are a senior oracle bone researcher who excels in classifying oracle bone characters.*
 716 *#User: Given the following two oracle bone characters, estimate the probability that they belong to*
 717 *the same class. Please return only a single integer between 0 and 100. <image1> <image2>*
 718 **“Yes-or-No” question template:**

719 *#System: You are a senior oracle bone researcher who excels in classifying oracle bone characters.*
 720 *#User: Whether these two oracle bone characters belong to the same class? Please return “Yes” or*
 721 *“No”. <image1> <image2>*

722 E.2 MODALITY CLASSIFICATION

724 “Which” question template:

725 *#System: You are a senior oracle bone researcher who excels in classifying the modality of oracle*
 726 *bone images.*
 727 *#User: Which modality is this oracle bone image belong to? <image1>*
 728 *A. Whole Rubbing Image.*
 729 *B. Whole Facsimile Image.*
 730 *C. Single Character Rubbing Image.*
 731 *D. Single Character Facsimile Image.*

732 E.3 DETECTION

734 “How” question template:

735 *#System: You are a senior oracle bone researcher who excels in detecting characters on oracle bone*
 736 *script images.*
 737 *#User: How many oracle bone characters are in this image? Please return the number of oracle*
 738 *bone characters in this image. <image1>*
 739 **“Where” question template:**

740 *#System: You are a senior oracle bone researcher who excels in detecting characters on oracle bone*
 741 *script images.*
 742 *#User: How many oracle bone characters are in this image? For each detected oracle bone char-*
 743 *acter, please return a bounding box in [xmin, ymin, xmax, ymax] format. <image1>*
 744 For “How” questions, we employ the relative counting error (MRE) metric to evaluate the performance of different LMMs:

$$745 \text{MRE} = \frac{1}{N} \sum_{i=1}^N \frac{|K_i^{gt} - K_i^{pre}|}{C_i^{gt}}, \quad (4)$$

749 where N is the number of evaluated OBS images. K_i^{gt} and K_i^{pre} represent the ground-truth and
 750 predicted numbers of oracle bone characters in the i -th OBS image, respectively.

752 E.4 GENERATION

754 For the facsimile image generation task, the input to our framework is a high-resolution rubbing
 755 image of an oracle bone inscription, which captures the raw visual appearance of the engraved
 characters along with the noise and texture artifacts introduced by the rubbing process. The objective

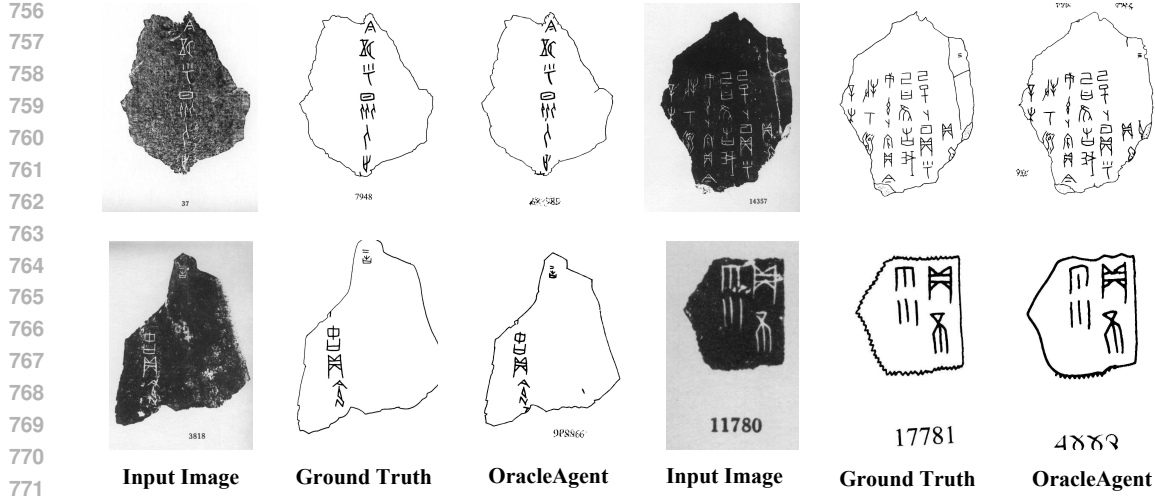


Figure 5: Examples of facsimile image generation. Note that input image is a rubbing image and OracleAgent generate its facsimile form.

is to transform this noisy archaeological input into a clean, interpretable facsimile representation suitable for scholarly analysis and publication.

As illustrated in Fig. 5, we present four representative examples of the complete generation pipeline. In each case, the left column shows the original rubbing image obtained from an actual oracle bone artifact. The middle column contains the ground-truth hand-drawn facsimile meticulously created by an epigraphic expert, which serves as the gold standard for accurate stroke reconstruction and character interpretation. The right column displays the facsimile automatically generated by OracleAgent, which aims to replicate the expert’s style and accuracy while removing background noise, cracks, and irrelevant visual artifacts.

This side-by-side comparison highlights OracleAgent’s ability to produce high-fidelity facsimiles that are visually and semantically consistent with expert renderings. The generated results not only preserve the structural integrity and stylistic characteristics of the oracle bone script but also significantly reduce the manual workload traditionally required for such tasks, thereby enabling scalable and efficient digital epigraphy.

F RETRIEVAL METRICS OF CASE STUDY

Given a set of ground truth results and predicted results for a specific retrieval task, the evaluation metrics are defined as follows:

Precision measures the proportion of correctly retrieved items among all retrieved items:

$$\text{Precision} = \frac{TP}{TP + FP} \quad (5)$$

where TP (True Positive) is the number of relevant items correctly retrieved, and FP (False Positive) is the number of irrelevant items incorrectly retrieved.

Recall measures the proportion of correctly retrieved items among all relevant items:

$$\text{Recall} = \frac{TP}{TP + FN} \quad (6)$$

where FN (False Negative) is the number of relevant items that were not retrieved.

F1-score is the harmonic mean of Precision and Recall:

$$\text{F1-score} = \frac{2 \times \text{Precision} \times \text{Recall}}{\text{Precision} + \text{Recall}} \quad (7)$$

864 fragment, only its presence is considered):
 865

$$866 \quad \text{Coverage} = \frac{|\text{Pred} \cap \text{Real}|}{|\text{Real}|} \quad (8)$$

$$867$$

868 where Pred is the set of predicted items and Real is the set of ground truth items.
 869

870 **G MORE EXAMPLES OF CASES STUDY.**

873 As shown in Fig. 6, we present representative user case studies illustrating OracleAgent’s ability to
 874 process diverse oracle bone script (OBS) inputs and queries. Inputs include rubbing images, cropped
 875 single-character segments, and cropped single-character facsimile, accompanied by user requests
 876 such as character identification, semantic interpretation, document retrieval, and clean facsimile
 877 generation. For each case, we show the user query, the system’s response, and the reasoning trace
 878 that reveals OracleAgent’s step-by-step decision process. These examples highlight the system’s
 879 versatility across various oracle bone modalities and its capability to deliver accurate, interpretable
 880 results for epigraphic research.

881 In summary, these case studies demonstrate that OracleAgent can effectively handle a wide range of
 882 input modalities and user queries in oracle bone script research. The system’s ability to provide ac-
 883 curate, interpretable, and context-aware responses highlights its potential to facilitate and accelerate
 884 epigraphic analysis. We believe OracleAgent represents a significant step toward the development
 885 of comprehensive AI-assisted tools for historical document interpretation.

886
 887
 888
 889
 890
 891
 892
 893
 894
 895
 896
 897
 898
 899
 900
 901
 902
 903
 904
 905
 906
 907
 908
 909
 910
 911
 912
 913
 914
 915
 916
 917